DIODE-LASER ABSORPTION MEASUREMENTS OF HYDRAZINE AND MONOMETHYLHYDRAZINE

M.E. Webber†, R.M. Mihalcea, D.S. Baer, and R.K. Hanson

High Temperature Gasdynamics Laboratory
Department of Mechanical Engineering
Stanford University, Stanford, CA 94305-3032

J. Segall and P.A. DeBarber

MetroLaser, Inc.
18010 Skypark Circle, Ste. 100
Irvine, CA 92614

Abstract

Absorption measurements of pure hydrazine, N_2H_4, and monomethylhydrazine, $CH_3N_2H_3$ (MMH), were recorded in an optical absorption cell (3 passes, 50 cm/pass) at low pressure (0-35 Torr) using a tunable external-cavity diode laser (ECDL), operating in the range from 6350 to 6650 cm^{-1} (1.49 μm to 1.58 μm). Peak absorption cross-section measurements of hydrazine and MMH, as determined from fixed wavelength absorption measurements, were found to be $\alpha_e(\nu)=0.163 \pm 0.008$ $cm^{-1}atm^{-1}$ at 6495 cm^{-1} (λ=1539.6 nm) and $\alpha_e(\nu)=0.152 \pm 0.003$ $cm^{-1}atm^{-1}$ at 6560 cm^{-1} (λ=1524.4 nm), respectively.

Introduction

Hydrazine and monomethylhydrazine (MMH) are hypergolic fuels used by NASA on the Space Shuttle for auxiliary power and orbital maneuvering systems. Because these species are toxic, carcinogenic and highly flammable and are loaded onto the space shuttle several weeks prior to launch, it is necessary to monitor for leaks during the pre-launch period. The present work is aimed at establishing the feasibility of a near-IR diode-laser absorption sensor system for non-intrusive species-specific concentration measurements of hydrazine-fuel vapors that might pose a serious health or explosion risk near the shuttle launchpad.

---

† Corresponding author.

Currently, NASA uses electrochemical sensors for hypergolic leak detection. Because of the possibility of sensor-induced ignition of hypergolic fuels, these sensors are located remotely and air samples are drawn to the electrochemical sensors through plastic sampling lines, thereby reducing the sensitivity due to adsorption onto the lines and greatly slowing the time response of the sensor system. A near-IR optical detection strategy was selected as a candidate for a new launchpad sensor for several reasons. Optical techniques offer the advantage that no electrical components (with potential sparks) need to be exposed to hydrazine vapors, reducing the fire and explosion risks in the event of a leak. Additionally, optical techniques are non-intrusive, allowing for accurate on-site measurements of hydrazine vapor presence without extractive probe systems. Moreover, optical detection in the near infrared spectral region enables the use of communications-grade fiber-optic components and thus offers the opportunity to use multiplexing strategies for making simultaneous measurements of multiple species in multiple locations.[1]

A measurement strategy based on absorption spectroscopy requires the accurate determination of important spectroscopic parameters of the target species as well as potentially interfering substances. The focus of the current work is to present survey spectra of hydrazine and MMH near 1.55 μm using a commercially available room-temperature diode laser and to accurately determine the pertinent absorption cross-sections. In addition, we also present simulated spectra of the potential interfering species, ammonia and water vapor. These spectroscopic measurements will form the basis for the determination of appropriate spectral regions for the detection and the design of an optical sensor system for fuel-leak detection on the space-shuttle launchpad.

Theory

The theoretical basis for the measurement strategy may be described by the Beer-Lambert relation

$$\frac{I}{I_o} = e^{-k_v L},$$

where k_v is the spectral absorption coefficient [cm^{-1}], L is the pathlength [cm], *I* is the transmitted intensity, and I_o is the incident (reference) intensity. Hydrazine and MMH lack fine spectral structure in the near infrared, so the absorption coefficient may be expressed $k_v = \alpha_e(\nu)P_i$, where $\alpha_e(\nu)$ is the temperature-dependent napierian absorption cross-

section [$cm^{-1}atm^{-1}$] and P_i is the partial pressure of the absorbing species [atm]. Thus, if the absorption cross-section $\alpha_e(\nu)$ has been determined, the partial pressure of the probed species may be measured spectroscopically using the relation:

$$P_i = \frac{-\ln\left(I/I_o\right)}{\alpha_e(\nu)L} .$$

Gas Handling Setup

Hydrazines are flammable, caustic, and toxic and are suspected mutagens and carcinogens. Hazardous exposure can occur through inhalation or through skin contact.[2] In addition, hydrazines decompose when exposed to metal and metal oxide surfaces, permeate through fluorocarbons, and readily adsorb onto most surfaces.[3] Therefore, these materials must be handled with care and experimental results must be scrutinized for possible artifacts resulting from decomposition or surface adsorption.

The gas-handling and optical-measurement systems were designed to minimize health and safety risks and to maintain the purity of the hydrazine samples (see Figure 1). Glass, Poly-flo, and Tygon tubing were used throughout the gas handling system. The use of stainless steel and other metals was minimized as they catalyze the decomposition of hydrazine into ammonia, nitrogen, and hydrogen.[2,3] The inconel diaphragm of the MKS 690 Baratron pressure gauge (1% full-scale accuracy) was located as far as practical from the optical absorption cell to slow the introduction of decomposition products into the optical probe region. In addition, Buna-N O-rings were used since hydrazine reacts strongly with Viton O-rings. The ends of the cell windows were heated to 45 °C with resistance-heating tape to minimize adsorption on the windows.

Hydrazine vapor samples were introduced to the quartz cell following a freeze-pump-thaw cycle. This cycle consisted of the following steps. First, the test cell was evacuated and isolated from the hydrazine storage flask with a high-vacuum Teflon valve. A 1-mL sample of liquid hydrazine or MMH (Aldrich) was extracted with a syringe or pipette from its storage bottle and placed into the glass flask, after which the entire flask was placed in a liquid N_2 bath (the freezing points for hydrazine and MMH are 275 and 221 K respectively).[2] After the sample was frozen, the

Teflon valve was opened and the air in the sample flask was evacuated. After the entire system was sufficiently pumped down, the hydrazine or MMH sample was allowed to thaw. The Teflon valve was used to control the sample pressures in the cell up to the room-temperature vapor pressures for hydrazine (14.2 Torr) and MMH (49.47 Torr).

We discovered that the commercially obtained hydrazine and MMH contained significant concentrations of dissolved ammonia (NH_3), presumably due to chemical decomposition. Vapor samples from hydrazine were found to contain more ammonia than those from MMH, which is consistent with the greater stability of MMH to heterogeneous decomposition. The first hydrazine vapor sample contained the highest concentration of ammonia, while the second and third samples contained smaller, yet still measurable amounts of ammonia, as is shown in Figure 2. Since ammonia has a high vapor pressure (P_{NH3} ~ 6000 Torr at room temperature), the ammonia contaminant in the glass flask predominantly existed in the gas phase above the liquid hydrazine sample at ambient temperatures. Therefore, the ammonia contaminant were effectively removed by withdrawing several vapor samples. Nominally, the fourth and successive samples contained negligible ammonia contamination.

The decomposition of the hydrazines into ammonia was catalyzed by gas interactions with metal surfaces in the gas handling system. These surfaces in the gas handling system included three stainless-steel fittings located close to the test cell and the inconel diaphragm of the pressure gauge that was attached to the system with stainless-steel tubing. The heterogeneous hydrazine decomposition can be written as:

$$3N_2H_4 \rightarrow 4(1-x)\,NH_3 + (1+2x)\,N_2 + 6xH_2,$$

where x varies between 0 and 1, depending on surface(s) and temperature.[4] For this particular setup, ammonia absorbance features became discernable about 30 minutes after a clean hydrazine sample was introduced. Figure 3 shows the absorbance for a sample immediately and one hour after its introduction to the system. Figure 3 also indicates a decrease in the total pressure after one hour due to adsorption onto the cell walls and other surfaces in the gas handling setup. The gas handling system was evacuated by diluting the hydrazine with N_2 and passing the vapors through a gas wash filled with 0.15-molar HCl solution to neutralize the hydrazines.

Optical Setup

The optical system was comprised of an external cavity diode laser (ECDL) with a tuning range from 1496.6 to 1582.3 nm and a 5 MHz linewidth, quartz cell (50 cm length, 2.54 cm diameter) with wedged windows (30' wedge, mounted at a 3° angle), appropriate beamsplitters, mirrors and lenses, and two InGaAs detectors for measuring reference and transmitted intensities (0.3-MHz bandwidth). The beam path was set up in a three-pass configuration to achieve an effective pathlength of 150 cm, as is shown in Figure 1.

The output intensity of the ECDL over the entire laser tuning range is shown in Figure 4. A regular fringe pattern due to interference between the front and back surfaces of the gain medium within the ECDL is readily apparent. By comparing the laser intensity curve in Figure 4 with the fringe pattern of a solid etalon with a known free spectral range (FSR=2.01 GHz), the FSR of the laser fringes was determined. Figure 5 shows the linear relationship between the laser and the solid etalon fringes. The laser etalon fringe spacing corresponded to 71.9 ± 0.3 solid etalon fringes and a FSR=4.821 ± 0.006 cm^{-1}. The inherent FSR of the laser output (reference trace) was thus used to conveniently convert transmitted intensity data traces from time domain to the frequency domain and obviated the use of a separate etalon transmission measurement during the hydrazine absorption measurements.

The output intensity of the ECDL over the entire laser tuning range showed a regular fringe pattern due to interference between the front and back surfaces of the gain medium within the ECDL. By comparing the laser's fringe pattern with the fringes of a solid etalon with a known free spectral range (FSR=2.01 GHz), the FSR of the laser fringes was determined. Figure 5 shows the linear relationship between the laser and the solid etalon fringes. The laser etalon fringe spacing corresponded to 71.9 ± 0.3 solid etalon fringes and a FSR=4.821 ± 0.006 cm^{-1}. The inherent FSR of the laser output (reference trace) was thus used to conveniently convert transmitted intensity data traces from time domain to the frequency domain and obviated the use of a separate etalon transmission measurement during the hydrazine absorption measurements.

Spectroscopy

The goal of this work was to verify or improve upon the previously measured near-IR spectroscopic data on hydrazine and MMH.[5-7] The most recent spectroscopic publication pertaining to hydrazine spectroscopy was by Giguère and Liu in 1952.[5] They were unable to make an assignment for hydrazine's spectral feature near 1.5 μm, but measured its peak decadic absorption cross-section at 6500 cm^{-1} to be $\alpha_{10}(\nu)^{\dagger}$=0.013 $cm^{-1}atm^{-1}$. For MMH, a spectroscopic study was published as recently as 1993 by Murray and Kurtz[6] in which the MMH features between 6560 and 6300 cm^{-1} were assigned to the $\Delta\nu$=2 overtones of three different N-H stretching fundamentals at 3317 cm^{-1}, 3245 cm^{-1} and 3177 cm^{-1}. The peak for MMH in the 1.5-μm region was found to be near 6560 ± 20 cm^{-1} with a decadic absorption cross-section of $\alpha_{10}(\nu)$=0.031 ± .006 $cm^{-1}atm^{-1}$.

In the present work, absorption survey spectra measurements of hydrazine and MMH in the optical cell were recorded by tuning the ECDL from 6350 cm^{-1} to 6650 cm^{-1} in a single sweep. Scans across the entire tuning range of the laser required approximately 3.5 minutes. For the scans, detector signals were passed through an SR640 Dual Channel anti-aliasing filter (f_{-3db}=5 Hz) and collected with a 12-bit Nicolet digital oscilloscope at a 20-Hz sampling frequency. The effective frequency resolution in the raw data, based on the data acquisition sampling frequency, was approximately 0.05 cm^{-1}.

The total pressure in the cell decreased slightly (typically less than 0.1 Torr/min) during the 3.5-minute-long survey scans (300 cm^{-1}) due to adsorption to the cell walls. Waiting for the adsorption to reach steady state was not a viable option for two reasons: 1) it was not clear if adsorption would reach steady state — the hydrazines could continue to permeate the Poly-flo and Teflon in the system indefinitely,[3] and 2) increased measurement time could lead to increased sample contamination due to chemical decomposition. Reference traces were recorded before and after filling the cell with hydrazine or MMH and compared with transmission traces to determine respective absorbances. Low-pass digital filters (f_{-3db} = 0.15 Hz) were applied to the measured transmission spectra to attenuate the laser cavity etalon fringes. Measurements of hydrazine and MMH absorbance at various pressures are shown in

---

† The decadic absorption cross-section, $\alpha_{10}(\nu)$, is related to the napierian absorption cross-section, $\alpha_e(\nu)$, by the following relation: $\alpha_e(\nu) = \alpha_{10}(\nu) \cdot \ell n(10) \approx 2.3026 \cdot \alpha_{10}(\nu)$.

Figures 6 and 7, respectively. Survey spectra of hydrazine and MMH taken under similar conditions, shown in Figure 8, allows comparison of the relative absorption intensity of the two species as a function of frequency. We find the peak absorbance for hydrazine at 6495 ± 2 cm^{-1}, in good agreement with previous spectroscopic work on hydrazine.[5] For MMH, our location of the absorption peak at 6560 ± 2 cm^{-1} agrees with that cited by Murray and Kurtz.[6] In addition, the present results are in excellent qualitative agreement with a previously measured MMH spectrum,[7] as is shown in Fig. 9.

The timescales that were involved for the survey spectra introduced the possibility of hydrazine or MMH decomposition inside the cell and thus limited the survey spectra accuracy to approximately ±10%. In order to improve the accuracy for absorption cross-section measurements at specific frequency locations (e.g. the broadband peaks), the ECDL wavelength was fixed and the absorption was observed at various pressures. For these fixed-wavelength studies, absorption measurements were typically made within approximately 1 minute after the introduction of hydrazine or MMH samples to the system, reducing the possibility of decomposition affecting the integrity of the data. Moreover, the data were collected over a period of less than 1 second, eliminating the effect of pressure changes during the measurement time due to adsorption. The fixed-wavelength measurements improved the measurement accuracy from approximately ±10% in the survey spectra to about ±2%. This estimated total uncertainty of ±2% for the fixed-wavelength measurements reflects our estimate of the gas handling system's ability to maintain and measure known pressures of pure hydrazine and MMH samples. The uncertainty for each absorption cross-section value given below reflects the ±2% accuracy for the gas handling system, along with the standard deviation in the measurement of that absorbance cross-section value.

The measured absorbance from the fixed-wavelength measurements were plotted versus pressure and a linear fit was performed on the data (see Figures 10 and 11). We note that if appreciable sample decomposition occurred during the period prior to the absorption measurements, each sample would have a somewhat different composition because of differences in the residence time in the system for each sample. This variability in composition would manifest itself as deviations from straight line behavior in the absorbance versus pressure plots. The high quality of the linear fits indicates that appreciable sample decomposition did not occur prior to the absorption measurements.

The slope of measured absorbance versus pressure was used to determine the product $\alpha_e(\nu)L$, and thus $\alpha_e(\nu)$ for a known pathlength L (in this case, 150 cm). The peak absorption cross-section for hydrazine was found at 6495 ± 2 cm^{-1} (λ=1539.6 nm) to be $\alpha_e(\nu) = 0.163 \pm 0.008$ cm^{-1}atm^{-1}. The absorption cross-section of hydrazine at the frequency corresponding to the peak MMH absorbance (ν =6560 cm^{-1}, λ=1524.4 nm) was measured to be $\alpha_e(\nu) = 0.140 \pm 0.003$ cm^{-1}atm^{-1}. The peak MMH absorption cross-section $\alpha_e(\nu) = 0.152 \pm 0.003$ cm^{-1}atm^{-1} occurs at 6560 ± 2 cm^{-1}, λ=1524.4 nm). These absorbance cross-section values for hydrazine and MMH agree with those derived from the survey spectra to within the estimated 10% uncertainty quoted above. The absorbance cross-section results are summarized and compared with previous work in Table 1.

Our value for the hydrazine peak absorption cross-section of $\alpha_e(\nu) = 0.163 \pm 0.008$ cm^{-1}atm^{-1} is approximately five times higher than the peak value cited at 6500 cm^{-1} by Giguère and Liu.[5] This discrepancy is in part attributable to the low resolution of this earlier study. Low experimental resolution will lead to lower apparent peak cross-section determinations if the measurement resolution is on the order of the width of the feature being measured. In addition, Giguère and Liu performed their study in a metal test cell, which likely resulted in hydrazine decomposition. Decomposition will also reduce the apparent absorption cross-section.

The peak absorption cross-section for MMH determined in the present work is approximately twice as large as that determined by Murray and Kurtz,[6] as shown in Table I. This discrepancy is well outside the combined estimated uncertainties of the two cross-section determinations and thus possible reasons for this discrepancy merit some discussion here. The MMH spectra shown in Figure 3 of Murray and Kurtz (Ref. 6) shows some sharp features or spikes on the short wavelength side of the largest MMH absorption band. These spikes, at approximately 1.51 μm, are very likely attributable to the ammonia lines that appear at that wavelength, as shown in Figures 2 and 3 of this work. This indicates that the samples used by Murray and Kurtz were either contaminated or that heterogeneous decomposition of the MMH occurred prior to the scan. The heterogeneous decomposition of MMH is even more complex than that of hydrazine, but it is likely that the products include CH_4, N_2 and H_2, which are not discernable in this spectral region. Heterogeneous decomposition would reduce the partial pressure of MMH and therefore reduce the apparent absorption cross-section. In addition, for the majority of their measurements, Murray and Kurtz relied on the assumption that the MMH vapor concentration had reached saturated vapor pressure when the measurements were made. This assumption might not have been valid, as the authors themselves note. However, Murray

and Kurtz also performed 2 measurements for which the vapor pressure of MMH was determined by measurement of mid-IR absorption, where the absorption cross-section has been determined previously, and the near-IR absorption cross-section values from these measurements are similar to the others determined by Murray and Kurtz. The reason for the discrepancy between these measurements and our work is not clear.

A reliable sensor must minimize the effects of spectral interferences from species that are likely to be present in the measurement environment. Water vapor is present in high concentration in ambient air and ammonia is used in space shuttle operations and therefore might also be present at the launchpad. Figure 12 displays the calculated absorbance due to 50-ppm of NH_3 and 35% relative humidity at room temperature, atmospheric pressure, and 1 cm pathlength in the same spectral region as the MMH and hydrazine.[8-10] It is clear that these species potentially interfere with an optical sensor in this spectral region. A spectrally narrow light source, such as a single-mode diode laser, operating at a carefully chosen wavelength would be suitable for use in an optical probe to avoid these interferences and allow species specific detection.

Total measurement noise due to laser amplitude noise and baseline drift may be avoided by using phase sensitive detection techniques. A minimum detectable absorption of 4×10^{-5} was achieved in a 1-second bandwidth by electrically modulating the laser current at 10 kHz and demodulating the photodetector voltage using a digital lock-in amplifier (SRS850). Thus, with the measured values of hydrazine and MMH absorption cross-sections ($\alpha_e(\nu) \approx 0.15$ $cm^{-1}atm^{-1}$), the minimum detectivity for this preliminary study is 3 ppm for a 1-meter pathlength and a 1-second time constant.

Conclusions

Gas phase absorption spectra for hydrazine and MMH in the spectral region 6350-6650 cm^{-1} were measured using an external cavity diode laser. The peak absorption cross-sections for hydrazine and MMH were found to be $\alpha_e(\nu)=0.163 \pm 0.008$ $cm^{-1}atm^{-1}$ at 1539.6 nm (6495 cm^{-1}) and $\alpha_e(\nu)=0.152 \pm 0.003$ $cm^{-1}atm^{-1}$ at 1524.4 nm (6560 cm^{-1}) respectively. The quoted uncertainties reflect the standard deviation in each measurement combined with an estimated ±2% accuracy for the fixed wavelength measurement technique used to determine peak absorption cross-sections. The estimated accuracy of absorption cross-sections as determined from the survey spectra is ±10%. Our

measured peak absorption cross-sections are higher than those in previously published work by a factor of five for hydrazine and a factor of two for MMH. The discrepancies may be due in part to inaccuracies in pressure estimations and chemical decomposition or contamination of the sample gases in the previous work. Based on a minimum detectable absorbance of $4\times10^{-5}/Hz^{½}$, the estimated minimum detectivity for the present measurement strategy is 3 ppm in a 1-meter path. The sensitivity of the absorption measurements illustrates the potential for a hydrazine vapor sensor based on near-IR diode-laser absorption spectroscopy.

Acknowledgments

We gratefully acknowledge the support of NASA contract No. NAS10-97004, with Dr. Dale Lueck as technical monitor.

References

1. D.S. Baer, M.E. Newfield, N. Gopaul, and R.K. Hanson, "Multiplexed diode-laser sensor system for simultaneous H_2O, O_2, and temperature measurements," *Optics Letters*, vol. 19, 1900-1902 (1994).
2. E.W. Schmidt, "Hydrazine and its Derivatives: Preparation, Properties and Applications," J. Wiley, New York, 1984.
3. N.B. Martin, D.D. Davis, J.E. Kilduff, and W.C. Mahone, "Environmental Fate of Hydrazine," Test report ESL-TR-89-32, Air Force Engineering and Services Center, Tyndall Air Force Base, FL (1989).
4. H. H. Sawin, "A Kinetic Study of Hydrazine Decomposition on Ir(111) by Molecular Beam Scattering and Temperature Programmed Decomposition", Ph.D. Thesis, Chem. Eng. University of California, Berkeley, 1980.
5. P.A. Giguere and I.D. Liu, "On the Infrared Spectrum of Hydrazine", *J. Chem Phys*, 20, p. 136, 1952.
6. M. Murray and J. Kurtz, "Near-Infrared Absorptions of Monomethylhydrazine", *J. Quant. Spect. Radiat. Transfer*, 50, p. 585, 1993.
7. D. Lueck to J. Segall, private communication, 1996.
8. L.S. Rothman, et al., "The 1996 HITRAN Molecular Spectroscopic Database and HAWKS (HITRAN Atmospheric Workstation)," *JQSRT* (in press).
9. L. Lundsberg-Nielsen, F. Heglund and F.M. Nicholaisen, "Analysis of the High-Resolution Spectrum of Ammonia ($^{14}NH_3$) in the Near-Infrared Region, 6400-6900 cm^{-1}", *J. Mol. Spec*. v162, p230, 1993.
10. L. Lundsberg-Nielsen, "Molecular Overtone Spectroscopy on Ammonia", Ph.D. Thesis, Department of Chemistry, Univ. of Copenhagen, 1995.

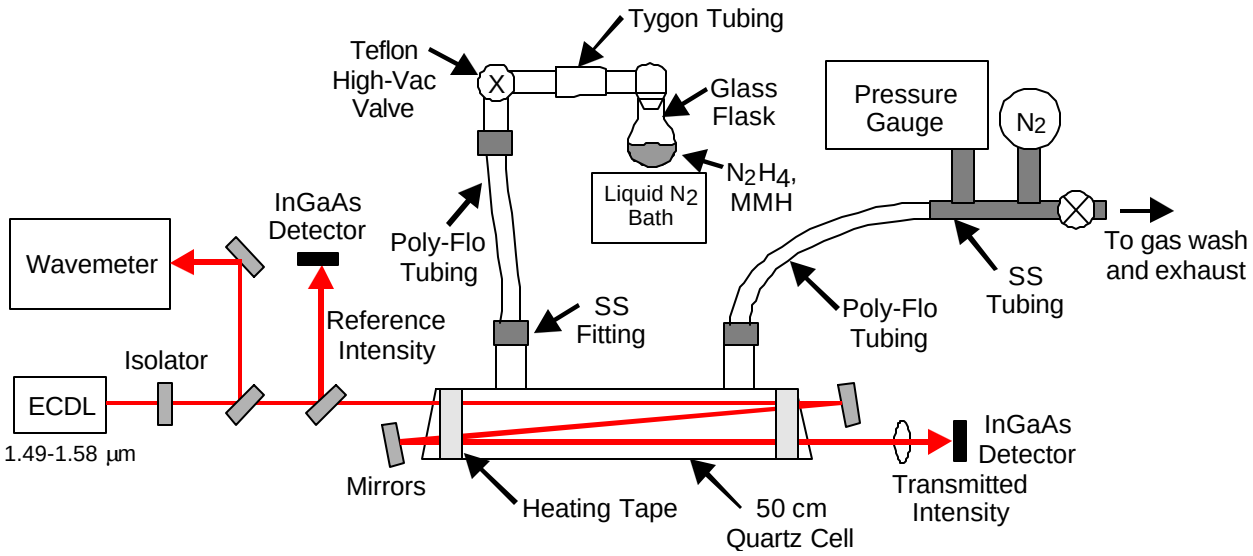

Fig. 1 Experimental schematic of the gas handling and optical measurement system.

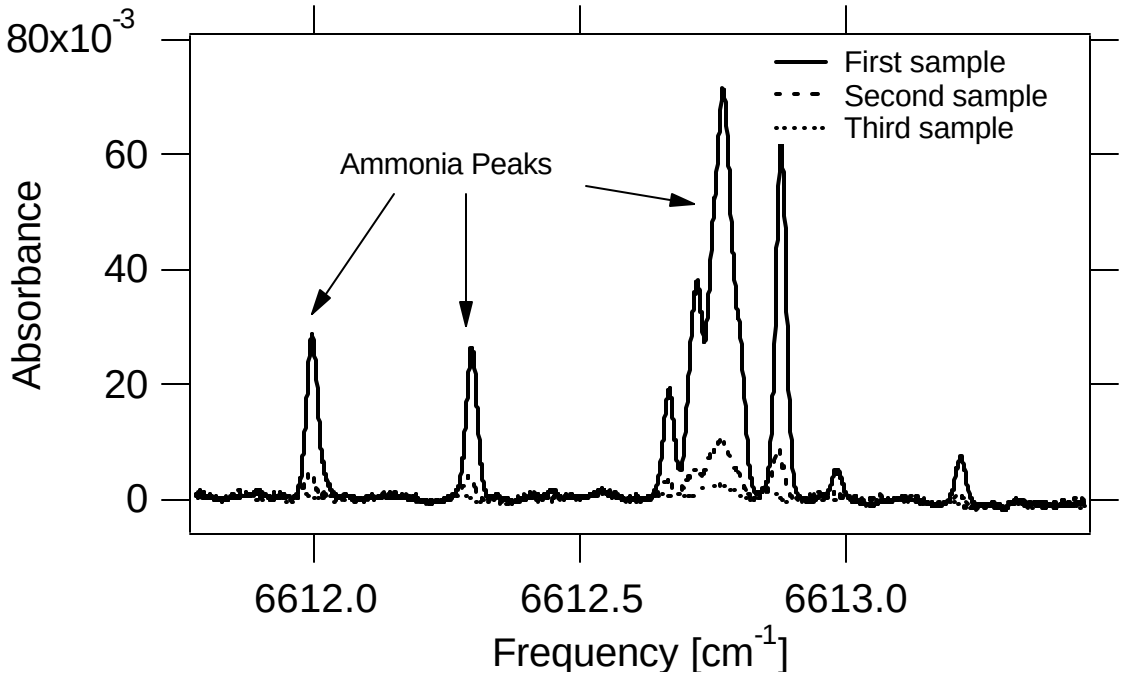

Fig 2. Ammonia absorbance recorded in sample cell (absorbance due to hydrazine has been subtracted) for the first three vapor samples obtained from the hydrazine supply.

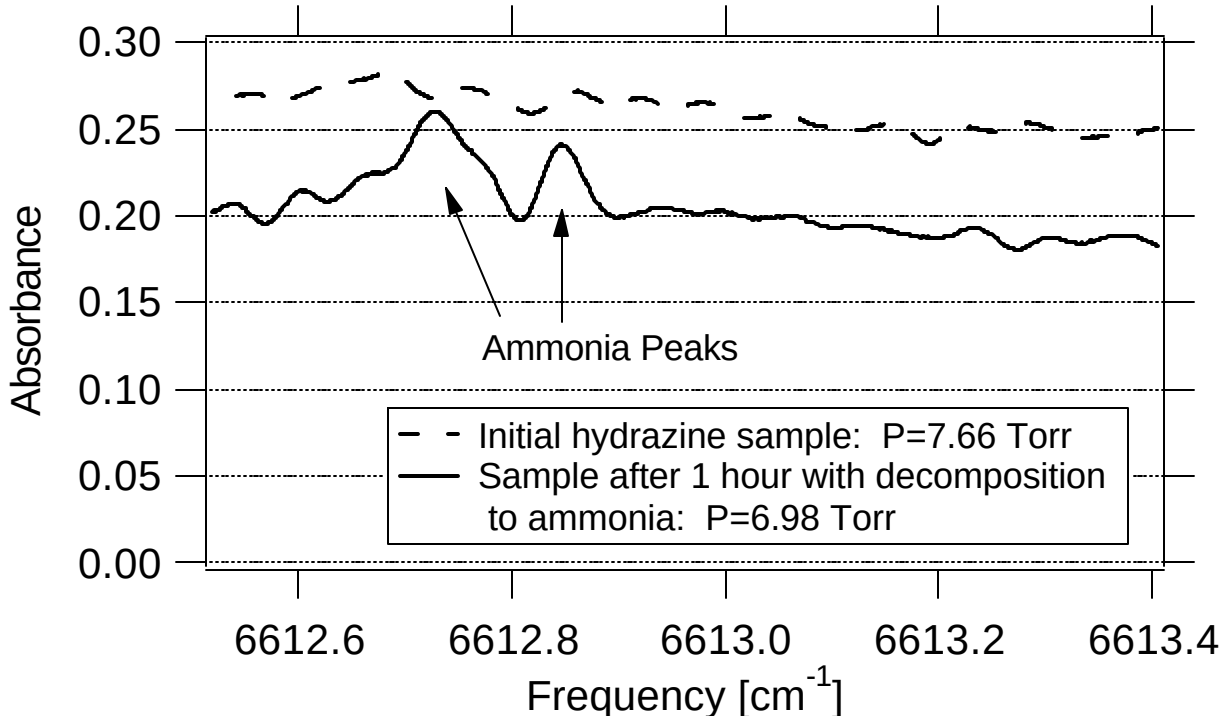

Fig 3. Measured hydrazine absorbance immediately (dashed line) and one hour (solid line) after introduction into the system. The decrease in total pressure is due to adsorption on the cell walls.

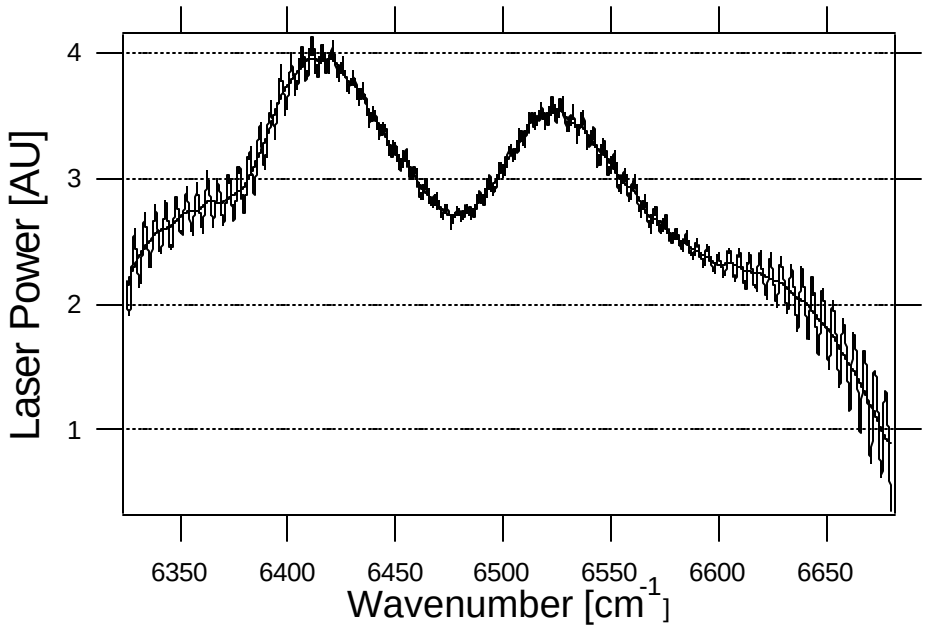

Fig 4. Output laser intensity over the entire tuning range. The maximum power is approximately 3.2 mW. The interference fringes are due to the finite reflectivity on the laser output facet. (Currently available ECDLs from the vendor have improved coatings that significantly reduce this effect.)

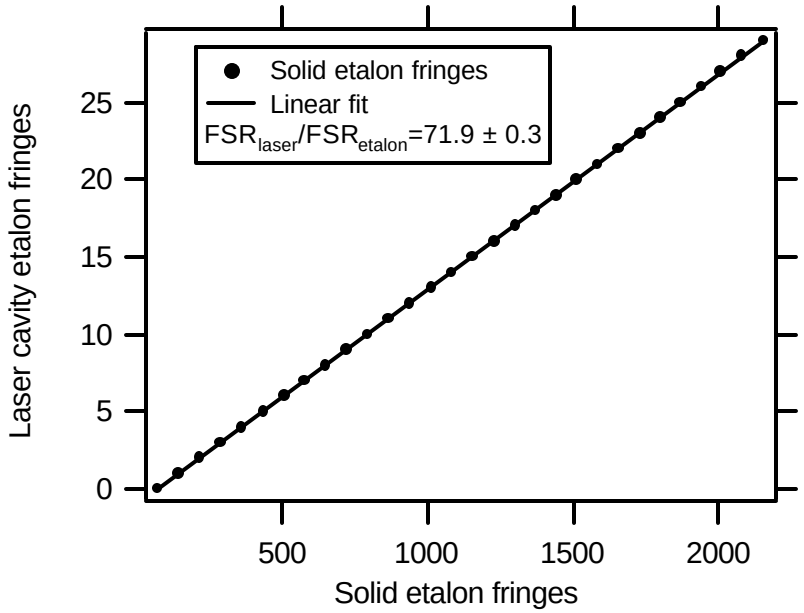

Fig 5. Comparison of the laser etalon fringes with those from solid etalon with a known free spectral (FSR=2.01 GHz).

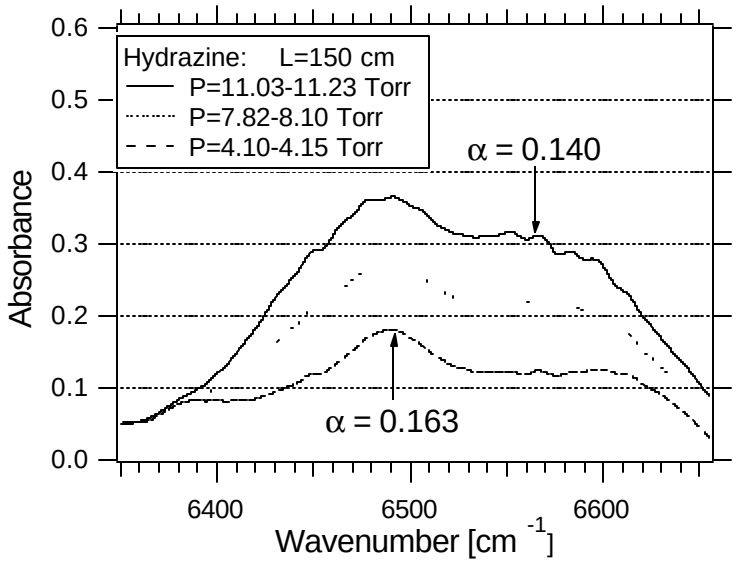

Fig 6. Hydrazine survey spectrum at three different pressure conditions. The pressure ranges listed are due to gas adsorption on the cell walls during a scan. The napierian absorption cross-sections are indicated at the hydrazine and MMH peak locations.

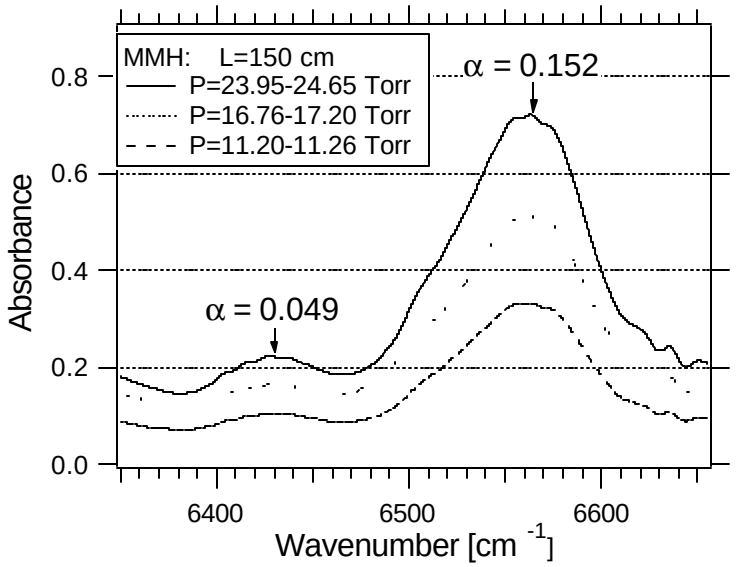

Fig 7. MMH survey spectrum at three pressures. The pressure ranges that are listed are a result of adsorption during the course of a scan. The napierian absorption cross-sections are indicated for the two MMH peak locations.

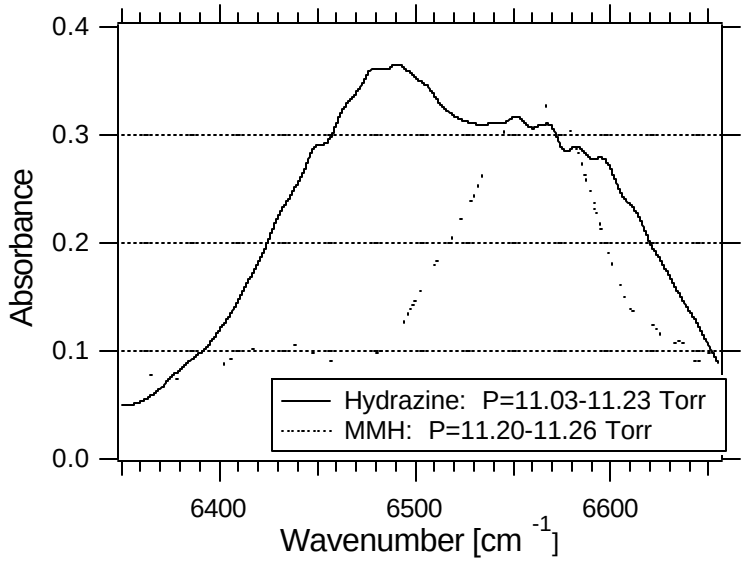

Fig 8. Measured MMH and hydrazine survey spectra at nominally similar conditions (P≈11 Torr; L=150 cm).

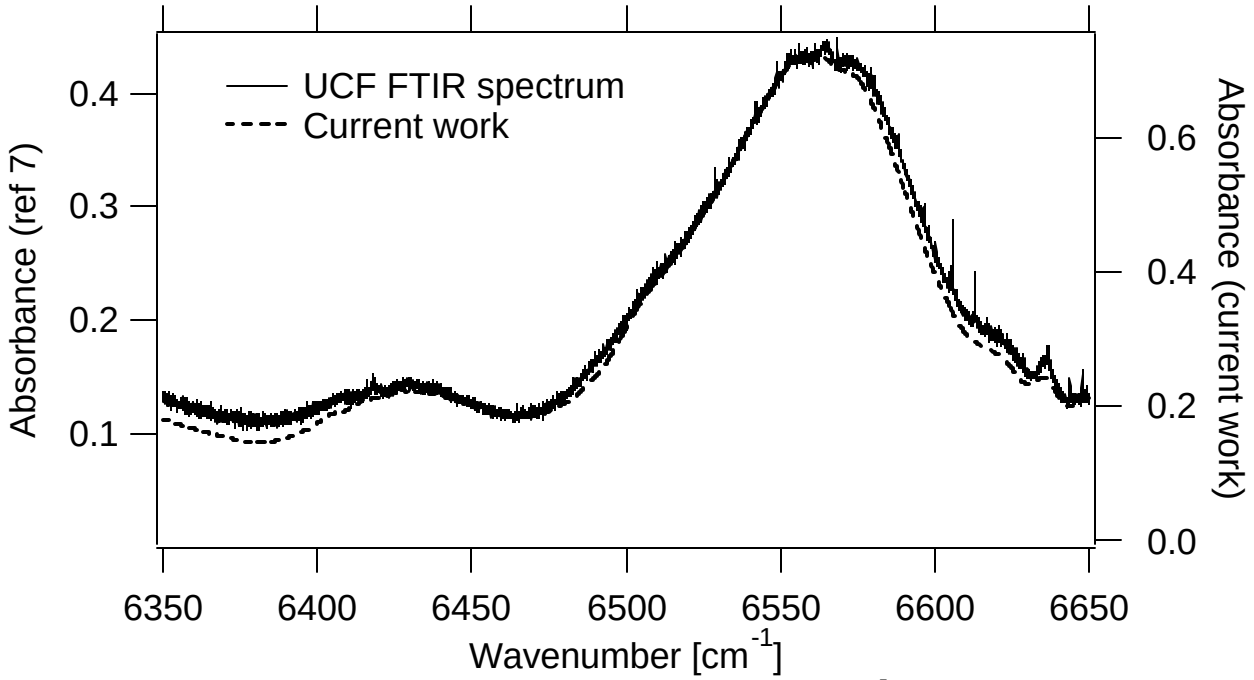

Fig 9. Comparison between current work and previous survey spectra of MMH.[7]

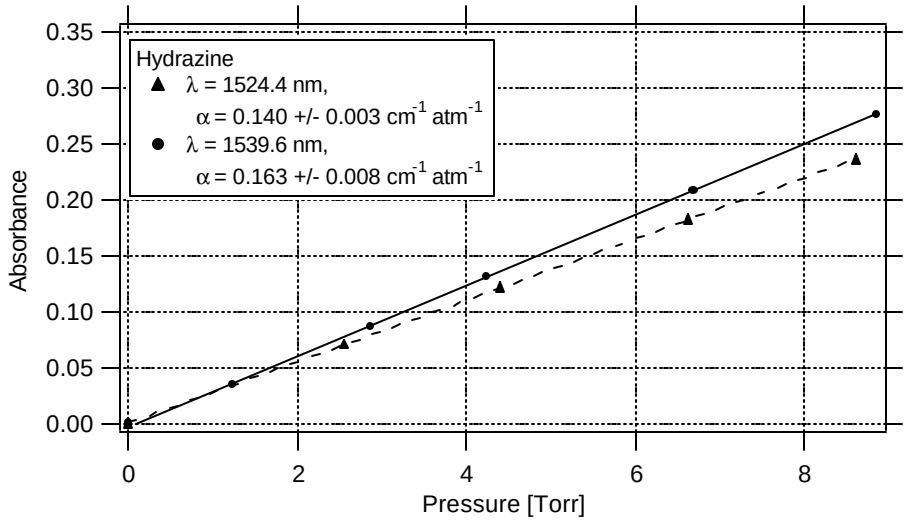

Fig 10. Linear hydrazine absorbance vs pressure at two wavelengths. The slope of the line and the pathlength determine $\alpha_e(\nu)$.

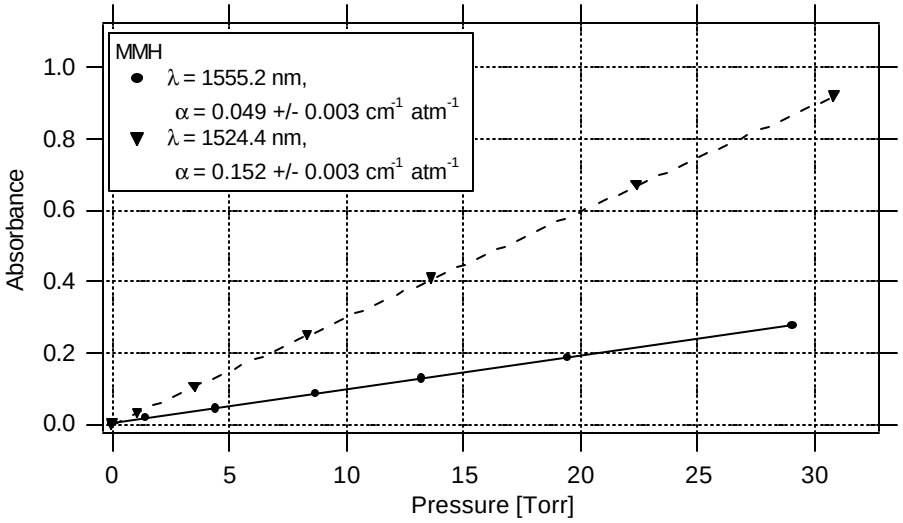

Fig 11. Linear MMH absorbance vs pressure at two fixed wavelength positions. The slope of the line and the pathlength determine $\alpha_e(\nu)$.

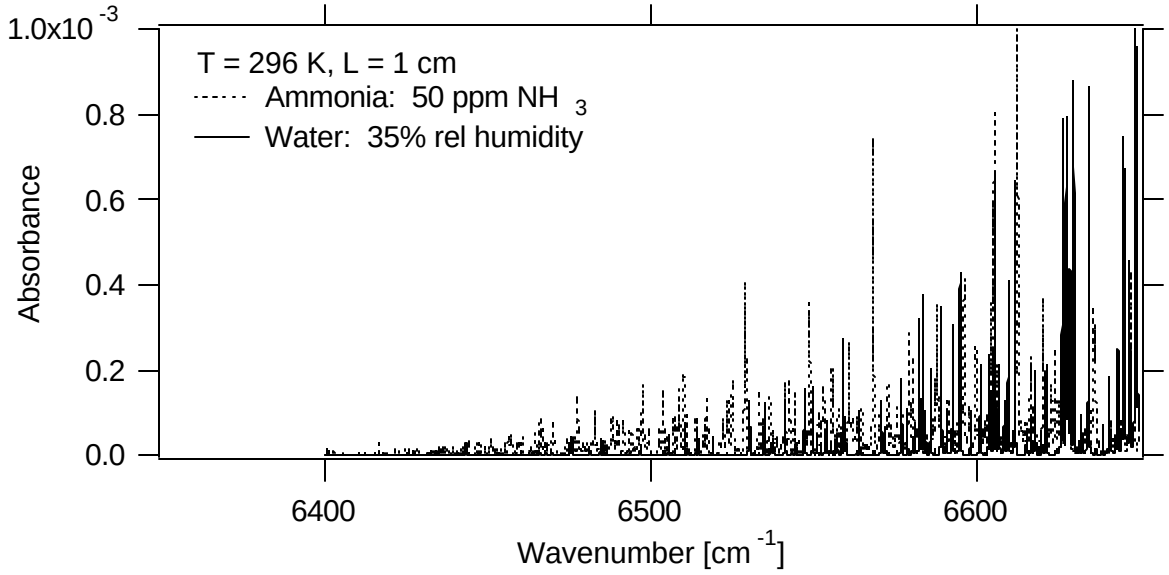

Fig 12. Absorption due to NH_3 (dashed line; 50 ppm) and H_2O (solid line; 35% relative humidity) in the probed spectral region near 1.5 μm.

Table 1. Comparison of hydrazine and MMH peak absorption cross-sections with previously published works.

	This work	Murray, et al[6]	
MMH peak	α_e [$cm^{-1}atm^{-1}$]	α_{10} [$cm^{-1}atm^{-1}$]	α_e [$cm^{-1}atm^{-1}$]
λ=1524.4 nm	0.152 ± 0.001	0.031	0.071
	This work	Giguère, et al[5]	
Hydrazine Peak	α_e [$cm^{-1}atm^{-1}$]	α_{10} [$cm^{-1}atm^{-1}$]	α_e [$cm^{-1}atm^{-1}$]
λ=1539.6 nm	0.163 ± 0.007	0.013	0.030